Nuclear Engineering and Technology 56 (2024) 4141–4148

Contents lists available at ScienceDirect

Nuclear Engineering and Technology

journal homepage: www.elsevier.com/locate/net

Original Article

Natural radioactivity, mineralogy and hazard assessment of syenogranites (ornamental stones) using a statistical approach

Sherif A. Taalab [a,**], Ahmed M. Ismail [b], W.M. El Maadawy [b], Kamal Abdelrahman [c], Mayeen Uddin Khandaker [d,e], Ahmed K. Sakr [f], Mohamed Y. Hanfi [b,g,*]

[a] Department of Geology, Faculty of Science, Al-Azhar University, Cairo, P.O. Box 11884, Egypt
[b] Nuclear Materials Authority, P.O. Box 530 El-Maadi, Cairo, Egypt
[c] Department of Geology and Geophysics, College of Science, King Saud Univ., P.O. Box 2455, Riyadh, 11451, Saudi Arabia
[d] Applied Physics and Radiation Technologies Group, CCDCU, School of Engineering and Technology, Sunway University, Bandar Sunway, 47500, Selangor, Malaysia
[e] Faculty of Graduate Studies, Daffodil International University, Daffodil Smart City, Birulia, Savar, Dhaka, 1216, Bangladesh
[f] Department of Chemistry and Biochemistry, The University of Hull, Kingston Upon Hull, HU6 7RX, UK
[g] Ural Federal University, Ekaterinburg, 620002, Russia

ARTICLE INFO

Keywords:
Granitic rocks
NaI (Tl) detector
Radionuclides
Radiological hazard
Uranophane

ABSTRACT

The study focused on syenogranite and its altered variety, and specifically monitored the activities of ^{226}Ra, ^{232}Th, and ^{40}K using NaI(Tl) gamma-ray spectroscopy. Syenogranites in the study area in Egypt were investigated to determine their potential use in industries such as ornamental stones and ceramics. The main outcrops in the study area consist of metasediments, metavolcanics, metagabbro, syn-to late-orogenic granites, and post-orogenic granites (syenogranites). There are also numerous dikes and veins of various shapes and compositions that have intruded and penetrated all the older rocks in the area. The mean activity (± standard deviation, SD) of these radioelements in the granites is ^{226}Ra (63 ± 71 Bq kg^{-1}), ^{232}Th (76 ± 170 Bq kg^{-1}), and ^{40}K (1248 ± 532 Bq kg^{-1}) were found to be greater than the world average. The radiological hazards are mostly attributed to the γ-rays emitted by granitic rocks. The granites studied in this study deviate from international standards mainly due to the presence of minerals containing radioelements such as zircon, allanite, monazite, sphene titanite, apatite, thorite, samarskite, fergusonite, xenotime, columbite, apatite and fluorite. As a result, granitic rocks are unsuitable for home building.

1. Introduction

Two major sources of natural radioactivity that affect our daily lives are terrestrial and cosmic radiation. External exposure occurs when individuals are exposed to gamma rays emitted by naturally occurring radionuclides like ^{238}U, ^{232}Th, and ^{40}K. On the other hand, internal exposure arises from inhaling radon gas [1–4]. In recent decades, numerous studies conducted worldwide have paid considerable attention to the analysis of health hazards associated with prolonged whole-body radiation exposure. However, different studies conducted worldwide have yielded different results regarding the presence of natural radioactivity in granite rocks, soils, and sediments [5–9]. Metasediments, metavolcanics, metagabbro and granitoids are the primary rock formations found in the defined study area. Extensive hydrothermal alteration has been identified in the petrographic and geochemical characteristics of syenogranites altered in the vicinity of Abu Furad [10]. Granites have a distinct commercial identity, exhibiting unique petrographic and technological characteristics, as well as indications of their country of origin [11,12]. Granites, widely used as architectural and aesthetic materials for both interior and exterior applications, are natural solid stones that require more robust machinery for cutting, shaping, and polishing than marble. The mineral assemblages and overall petrologic characteristics of granitic rocks are closely linked to the levels of uranium, thorium, and potassium found within them [13,14]. Uranium and thorium are commonly found in apatite, titanite, and zircon in igneous and metamorphic rocks. Other highly radioactive natural minerals include uraninite and thorite, although they are insignificant components of rocks. Near the Earth's surface, uranium

* Corresponding author. Ural Federal University, Ekaterinburg, 620002, Russia.
** Corresponding author. Department of Geology, Faculty of Science, Al-Azhar University, Cairo, P.O. Box 11884, Egypt.
E-mail address: mokhamed.khanfi@urfu.ru (M.Y. Hanfi).

https://doi.org/10.1016/j.net.2024.05.017
Received 10 January 2024; Received in revised form 8 May 2024; Accepted 15 May 2024
Available online 23 May 2024

exhibits high mobility compared to thorium, which remains relatively stable. Uranium oxidizes to a water-soluble form that can be easily leached from rocks and then redeposited in sediments thousands of miles away. On the flip side, thorium has a significantly lower solubility than uranium and potassium, meaning it can only be transported through mechanical means like wind or weathering [11,15]. Abundant in felsic rocks, both thorium and uranium exhibit varying amounts that are influenced by the alkalinity or acidity. Pegmatites, in particular, showcase the highest concentrations. The acidity of rocks plays a role in increasing the potassium content. Through the analysis of radionuclides' natural levels and distributions in rocks and soils, we can enhance our comprehension of the radiological implications associated with these elements. When considering the construction of residential structures on soil and rock, it is of utmost importance to carefully assess the potential radiological hazards and their impact on human health [16,17]. Most naturally occurring radioactive materials (NORMs) are commonly found in geological formations and soil compositions and exist at levels considered safe for humans and the surrounding ecosystem [18,19]. However, due to geological transformations, certain areas have comparatively elevated natural levels of U, Ra, and Th. In regions characterized by elevated background concentrations, the mobilization of both natural and man-made radionuclides occurs rapidly [20,21]. The radioactive isotopes U and Th have a prolonged lifespan and give rise to various radioactive progeny products, which can potentially pose risks to both public health and the environment. The main contributor to radiation exposure among the general population is natural radiation. To effectively evaluate potential environmental risks, it is imperative to identify regions with elevated levels of natural background radiation and determine the necessary remediation measures. This necessitates quantifying the levels of radioactive background radiation [22,23]. The present study attempts to examine the radioactivity and mineralogy of syenogranites and to determine their environmental impact. Furthermore, this current research aims to evaluate the potential exposure to gamma rays emanating from these granitic formations. The identification of radioactive hazards is done by estimating various parameters related to radiological hazards.

2. Materials and methods

2.1. Geological setting

The investigated area is situated in Egypt's Central Eastern Desert. It

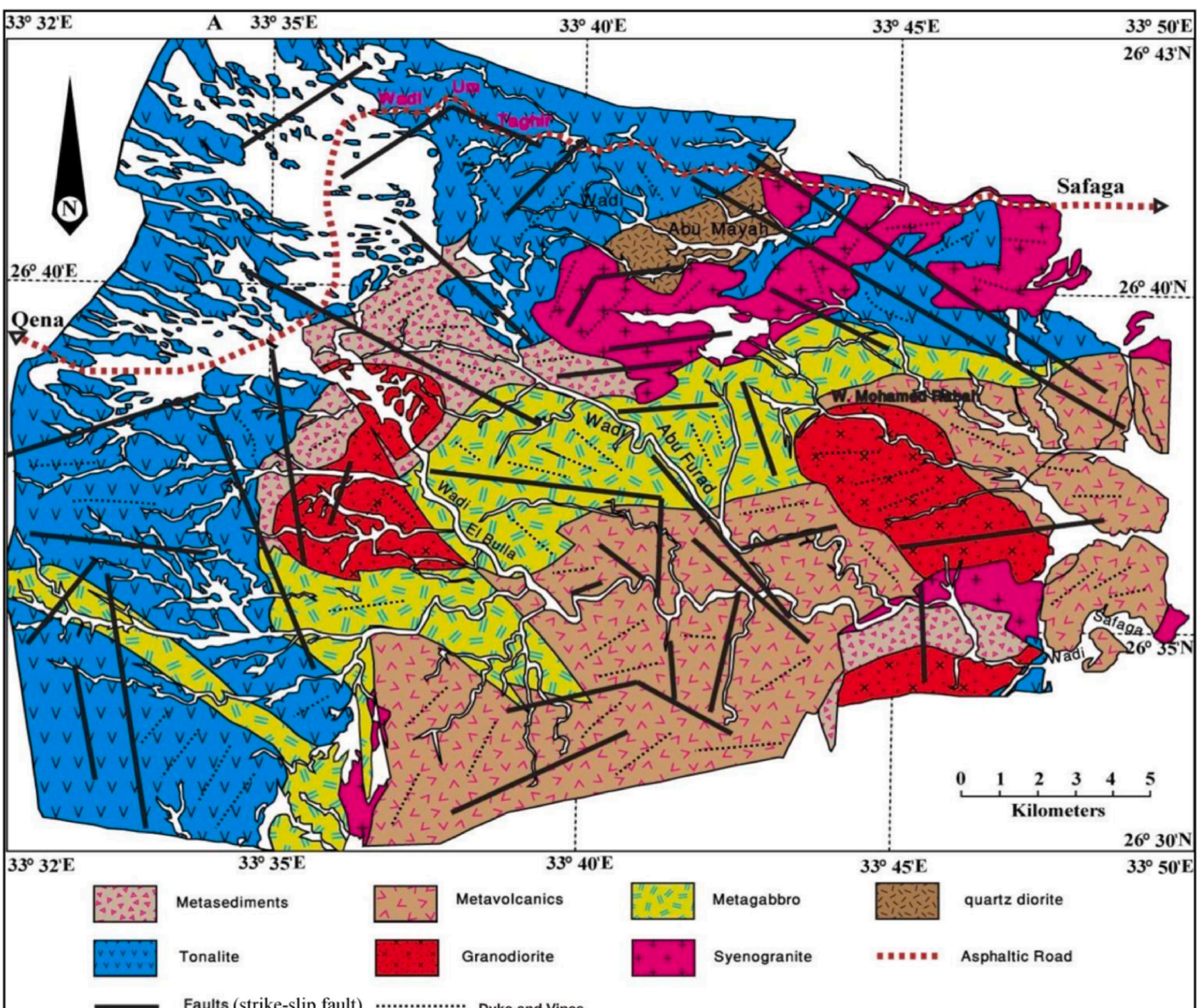

Fig. 1. Geologic map of the Gabal Abu Furad area Central Eastern Desert, Egypt.

spans 350 square kilometers of crystalline foundation rocks. It is located at coordinates Latitudes 26° 35′ 20" - 26° 43′32" N and Longitudes 33° 36′ 35" and 33° 47′ 27" E (Fig. 1) after [24].

2.2. Sample collection, preparation, and experimental techniques

Twenty syenogranite samples were collected from the Abu Furad area. Each sample weighed approximately 250 g and was carefully transported to the Nuclear and Radiological Regulatory Authority in Cairo. Upon arrival, they were immediately examined in the Radiation Protection Laboratory while being securely stored in properly labeled polyethylene bags. To ensure accurate analysis, the samples were air dried for 72 h at a temperature of 100 °C. The dried sample was subsequently divided into four equal parts, weighed, and then transferred to polyethylene Marinelli beakers with a capacity of 200 ml. These beakers were sealed and stored for approximately 28 days to establish secular equilibrium before undergoing radiometric analysis.

Monitoring the concentrations of radioactive elements (^{226}Ra, ^{232}Th, and ^{40}K) in the granite specimens involved the use of a scintillating NaI (Tl) gamma-ray analyzer equipped with a crystal phase measuring 7.6 cm × 7.6 cm. To ensure accurate readings, a cylindrical lead shield measuring 15.7 cm in diameter, 20.5 cm in length, and 3.7 cm in thickness was employed to shield the detector. The pulse data acquisition and analysis were facilitated by a spectroscopy amplifier and a multi-channel analyzer integrated into the management equipment. The devices were linked to a computer operating the SPTR-ATC software (AT-1315). The FWHM on energy peaks are explained in the manuscript. The following paragraph is added: "The net counts within the photo peak corresponding to the gamma energies are subsequently utilized for calculating the Full width and half maximum (FWHM). The gamma energies of the radionuclides under review for computing are as mentioned below. The activity concentration of ^{226}Ra was determined using the net counts under the 1.764 MeV photopeak (abundance: 15.30 %) emitted by its short-lived decay product, ^{214}Bi. The activity of ^{232}Th was determined using the net counts under the 2.614 MeV photopeak (abundance: 99.754 %) emitted by ^{208}Tl. The measurement provided is solely indicative of the concentration of uranium and thorium when there is a state of secular equilibrium between U-238, Th-232 and their various daughter isotopes. The activity of ^{40}K was determined using its own 1460 keV photopeak (abundance: 10.66 %) [25,26]. The usage of certified standard materials, like RGU-1 for ^{238}U, RGTh-1 for ^{232}Th, and RGK-1 for ^{40}K, is done in quantities that are comparable to the construction materials [27–29]. The minimum detection activity (MDAs) employed for samples recorded up to 20000 s are 2 Bq kg^{-1} for ^{226}Ra, 4 Bq kg^{-1} for ^{232}Th, and 12 Bq kg^{-1} for ^{40}K. The overall uncertainty of radiation levels is determined by applying the deviation equation, which incorporates both regular and stochastic misspecification. During the efficiency calibration, radioactivity readings exhibit systematic uncertainties ranging from 0.5 to 2 percent, in addition to up to 5 percent randomness [30].

After assessing the activity concentrations of ^{238}U, ^{232}Th, and ^{40}K, the radiological variables are computed to determine radioactivity measurement values. The estimation of the radiological variables is carried out according to the following.

The radium equivalent content (Raeq) is extensively used as a radioactive parameter in the assessment of radiation health hazards. It is vital to ensure that the Raeq data remains below 370 Bq kg^{-1}, as this helps to keep the annual effective dose (AED) for the public below one mSv. The Raeq can be calculated using the following formula [31]:

$$Ra_{eq}\ (\mathrm{Bq\ kg^{-1}}) = A_{Ra} + 1.43\ A_{Th} + 0.077\ A_K \quad (1)$$

The evaluation of gamma radiation's impact at a distance of 1 m from radiation sources in the air was carried out using the absorbed dose rate, a radioactive factor, taking into account the concentrations of ^{238}U, ^{232}Th, and ^{40}K [31].

$$D_{air}\ (\mathrm{nGy\ h^{-1}}) = 0.430\ A_U + 0.666\ A_{Th} + 0.042\ A_K \quad (2)$$

The annual effective dose, encompassing both outdoor and indoor radioactivity, is utilized as a means to assess radiation exposure levels over a fixed period of one year [32].

$$AED_{out}\ (\mathrm{mSv/y}) = D_{air}\ (\mathrm{nGy/h}) \times 0.2 \times 8760\ (\mathrm{h/y}) \times 0.7\ (\mathrm{Sv/Gy}) \times 10^{-6}\ (\mathrm{mSv/nGy}) \quad (3)$$

$$AED_{in}\ (\mathrm{mSv/y}) = D_{air}\ (\mathrm{nGy/h}) \times 0.8 \times 8760\ (\mathrm{h/y}) \times 0.7\ (\mathrm{Sv/Gy}) \times 10^{-6}\ (\mathrm{mSv/nGy}) \quad (4)$$

The external hazard index serves as a set of radiological parameters used to assess the risk of gamma radiation, whereas the internal hazard index is specifically employed for evaluating the exposure to radon and its decay products internally [33].

$$H_{ex} = \frac{A_U}{370} + \frac{A_{Th}}{259} + + \frac{A_K}{4810} \quad (5)$$

$$H_{in} = \frac{A_U}{185} + \frac{A_{Th}}{259} + + \frac{A_K}{4810} \quad (6)$$

Recognizing the diverse combinations of unique natural activities within the sample, a team of specialists suggested an alternative index to determine the magnitude of radiation hazard associated with the natural radionuclides in the samples.

$$I_\gamma = \frac{A_{Ra}}{150} + \frac{A_{Th}}{100} + + \frac{A_K}{1500} \quad (7)$$

The calculation of gamma radiation doses absorbed by the gonads is facilitated by the use of the yearly gonadal dose equivalent, a radioactive measure.

$$AGDE\ (\mathrm{mSv\ y^{-1}}) = 3.09A_{Ra} + 4.18A_{Th} + 0.314A_K \quad (8)$$

The term excess lifetime cancer refers to the radioactive factor that is employed to determine if gamma radiation exposure caused deadly cancer [34]. RF is risk factor (0.05 Sv^{-1}) and DL is duration time (70 years)

$$ELCR = AED_{out} \times DL \times RF \quad (9)$$

Separation of heavy minerals based on their magnetic susceptibilities was carried out using the Frantz Isodynamic Magnetic Separator (Model LB-1). The segregated minerals were then identified using a stereomicroscope and analyzed with an Environmental Scanning Electron Microscope (ESEM, Phillips XL-30) at the Nuclear Materials Authority (NMA). The ESEM analysis employed a 25–30 keV electron beam with a diameter of 1–2 mm, and a counting duration of 60–120 s. For certain selected regions surrounding the centers of the mineral grains, SEM-EDX investigations were conducted, lasting 180 s. Furthermore, the morphological characteristics of these minerals were also scrutinized using SEM-EDX.

3. Results and discussion

3.1. Mineral analysis

Studying the altered syenogranite is crucial in terms of mineralogy. Secondary uranium minerals, indicated as uranophane [Ca $(UO_2)_2(SiO_3OH)_2.5H_2O$], were the most commonly discovered accessory minerals. Uranothorite [(Th, U) SiO4] represents radioactive minerals. Zircon represents radioactive and rare-earth-bearing minerals ($ZrSiO_4$).

3.1.1. Secondary uranium minerals

3.1.1.1. Uranophane [Ca $(UO_2)_2(SiO_3OH)_2.5H_2O$]. In environments rich in Si^{4+}, uranium ore deposits undergo oxidation-hydration weathering, resulting in the formation of uranium silicate known as Uranophane. This calcium-based mineral is predominantly found in the oxidation zones of these deposits [35,36]. Generally, this mineral exists as perfect needle-like single crystals. Seven (O) anions coordinate the U^{6+} ions to form pentagonal bipyramids typical of this cation. As a result, calcium can be freed from changed oligoclase and calcite, while silica can be liberated from feldspars via kaolinization.

Ca^{+2}+2 UO_2+ 2SiO_2+ 6H_2O +3O_2–Ca $(UO_2)_2$↔Si_2O_7 .6H_2O

Various shades of yellow, including canary, lemon, orange-yellow, and straw yellow, offer different luster and hardness levels ranging from 2 to 3 on the Mohs scale. Uranophane grains are typically found in massive, soft, radiated aggregates with microfractures filling or coating feldspars. The crystals of Uranophane have poorly developed faces, making it difficult to obtain accurate morphological measurements using a binocular microscope (refer to Fig. S1a). They have weakly developed faces. Therefore, they are challenging to quantify images (Fig. S1a) morphologically. U (42.87 %), Si (38.64 %), Al (12.68 %), Ca (3.42 %), and K (2.39 %) are the primary components of uranophane grains, EDAX analysis, and BSE (Fig. S1a). Secondary enrichment of Fe can be seen in uranophane crystals. It could be due to Fe acting as a surrogate for Ca in the interaction of mineralized fluids at a later stage. In chemical investigations of uranophane [37], found significant quantities of Fe. The XRD pattern of Uranophane material reveals its typical d-spacing (7.80, 3.95, and 2.99 A^o) peaks at 2 Θ (11.33^o, 22.94^o, and 29.78^o) (Fig. S1b).

3.1.2. Radio and rare-earth bearing minerals

3.1.2.1. Zircon ($ZrSiO_4$). Zircon, a widely occurring accessory mineral, is commonly found in plutonic igneous rocks. The metamict state in zircon can be attributed to the presence of radioactive atoms. Zircon appears as short and long euhedral prismatic crystals under a binocular microscope, with various colors (pale yellow and reddish brown) (Fig. S1c) and is usually translucent to opaque. SEM analysis and BSE reveal that zircon grains are primarily comprised of Si (12.94 %), Al (2.68 %), U (4.67 %), Zr (65.36 %), and Hf (4.69 %), Fe (5.04 %) and Th (4.62 %). The radiation damage caused by the presence of U and Th in zircon crystals may be responsible for the darkening of zircon's color. Only zircon crystals contain U, indicating a secondary hydrothermal metamorphic source rather than a magmatic origin. The XRD pattern of zircon reveals its typical d-spacing peaks (3.32, 2.53, and 1.72 Ao) at 2Theta (26.85o, 35.39o, and 53.24o) (Fig. S1d).

3.1.3. Radioactive minerals

3.1.3.1. Uranothorite [(Th, U) SiO_4]. Uranothorite is a thorium silicate mineral that is found in high abundance. Uranothorite occurs as subhedral to anhedral, rounded to subrounded grains varying in color from yellowish-brown to dark yellow-brown with vitreous or resinous luster. The main components of uranothorite grains are U (10.14 %), Si (55.65 %), Al (8.36 %), Th (16.52 %), and Y (9.33 %), according to SEM analysis, and BSE (Fig. S1e). The XRD pattern of Thorite, an uranium mineral, exhibits its unique d-spacing peaks (3.57, 4.73, and 2.67 A^o) at 2Theta (24.83^o, 18.75^o, and 33.50^o) (Fig. S1f).

3.2. Radioelements distribution

The concentrations of radionuclides in the examined granitic rocks are given in Table S1. For uranium (eU), thorium (eTh), radium equivalent uranium (eRa), and potassium, the radioelement levels are (1.2–54.6 ppm), (2.2–188.6 ppm), (1.7–29.9 ppm), and (0.69–7.3 %), with averages of 6.93, 18.73, 5.65 ppm, and 3.99 percent, respectively. These granites are classified as nonuraniferous by Refs. [38,39], who described uraniferous granites as containing at least twice the Clark level of uranium (4 ppm) [40,41], excluding samples 14, 17, and 19, which are categorized as uraniferous. The uranium enrichment and depletion in these granites could be linked to uranium mobility in granites or nearby rocks. Because of uranium enrichment in some samples, the eTh/eU of the examined rocks (2.14) is lower than the natural ratio (3.5) for granitic rocks. The migration parameter (eU-eTh/3.5) ranges from −1.73 to 3.64, with an average of 1.44, indicating uranium migration with authigenic uranium.

3.3. Geochemistry of uranium and thorium

The inter-element correlations could be used to determine the source of radioactive mineralization. The examined granites' eU-eTh crosscuts exhibit a high positive association, implying that magmatic processes are crucial in uranium mineralization (Fig. S2a). On the other hand, eU and eTh have an ill-defined relationship, with eTh/eU highlighting the involvement of post-magmatic processes in uranium and thorium mobilization in isolation due to variations in exothermic circumstances [42], (Fig. S2b and c). eU and eTh show an ill-defined K percent relationship, which could be related to the lack of U and Th mobilization during the alteration of feldspars to clay minerals [11], (Fig. S2d and e). The eTh/K - eTh/eU relationship, which distinguishes between leached and fixed uranium, shows that specific samples are in the leached uranium sector while others are in the fixed uranium sector (Fig. S2f) [37,43].

3.4. Radioactive equilibrium

The calculated equilibrium factor ($P = eU/Ra\ (eU)$), which is the proportion of uranium concentrations (eU) to radium concentration Ra (eU), can be used to estimate the radioactive equilibrium of examined granitic rocks [42]. The P factors of the examined granitic rocks varied from 0.3 to 2.7, with an average of 0.84, which is less than 1 (Table S1 and Fig. S2g), indicating U-decay disequilibrium owing to uranium leaching from these rocks.

3.5. Radioactive analysis

The activity concentrations of ^{226}Ra, ^{232}Th, and ^{40}K were observed in both the syenogranite and altered syenogranite samples (Table S2). According to Table S2, the average activity concentrations of ^{226}Ra, ^{232}Th, and ^{40}K are 63 ± 71, 76 ± 170, and 1248 ± 532 Bq kg^{-1}, respectively. These values exceed the globally recommended limits of 32, 45, and 412 Bq kg^{-1} [1]. The activity concentrations of ^{226}Ra ranged from 19 to 332 Bq kg^{-1}. The minimum and maximum values of ^{232}Th were 9 and 766 Bq kg^{-1}, respectively. Additionally, the variation in ^{40}K values was observed between 216 and 2285 Bq kg^{-1}. The investigated granites displayed remarkably high activity concentrations of ^{226}Ra, ^{232}Th, and ^{40}K, making it a matter of considerable importance. This elevated radioactivity can be attributed to the presence of zircon, uranophane, uranothorite, thorite, fergusonite, samarskite, columbite, xenotime, apatite, and fluorite in the altered granite [10]. The analysis of descriptive statistics was carried out to offer an overview of the distribution of values, the asymmetric nature of the distribution, and the peakness for ^{226}Ra, ^{232}Th, and ^{40}K, as well as the variability (Table S2). Key statistical parameters like skewness, kurtosis, and coefficient of variance were employed. An asymmetrical distribution's head is denoted by positive skewness values, whereas negative values denote its tail. The activity concentrations of ^{226}Ra and ^{232}Th display asymmetry in their distributions, with ^{226}Ra showing a tail-oriented asymmetrical distribution. The kurtosis values indicate the maximum probability point in the distribution. For ^{226}Ra and ^{232}Th activity concentrations in the studied area, the kurtosis values are positive (+ve), signifying a distribution likelihood at its apex. The probability distribution for ^{40}K activity concentrations, on the other hand, exhibits flatness (−0.3). Table 1 clarifies that the mean values of ^{226}Ra and ^{232}Th are lower than

Table 1
Descriptive statistics of studied granites.

	N	Median	Skewness	Kurtosis	CV, %
^{226}Ra	20	39	3.2	11.3	114
^{232}Th	20	21	3.9	16.0	224
^{40}K	20	1370	−0.2	−0.3	43

the standard deviation (SD) values, thus resulting in high non-uniformity.

In contrast, the uniformity degree is achieved at ^{40}K. Additionally, Table 1 includes the presentation of the coefficient of variance (CV), revealing remarkably high values of 114 % and 224 % for ^{226}Ra and ^{232}Th, respectively. In contrast, the examined area displays only a moderate level of variability with ^{40}K, measuring at 43 %. The variation observed in the investigated areas is directly influenced by the granites present, which also serve as host minerals for ^{238}U and ^{232}Th. The distribution of activity concentrations for ^{226}Ra, ^{232}Th, and ^{40}K in the investigated area can be observed in Fig. 2 (a, b, c). It is anticipated that the activity concentrations of ^{40}K in the studied area will conform to a normal distribution, whereas a multimodality distribution is predicted for ^{226}Ra and ^{232}Th.

The analysis of data and creation of histograms were conducted using a multivariate statistical approach. IBM-SPSS version 21.0, a commercial statistics program, was utilized for these tasks. The normality of the findings was evaluated through the Kolmogorov-Smirnov (KS) test, as illustrated in Table S3. The KS test, assuming the null hypothesis, indicates that the distribution of natural radionuclide activity in granitoid rocks is consistent with normality. This finding specifically relates to the activity concentrations of ^{40}K, as all p-values obtained from the tests were higher than 1 %.

The activity concentrations of ^{226}Ra, ^{232}Th, and ^{40}K in granitic rock samples were assessed and compared to data from earlier studies (Table S4). The results indicate that the levels of these elements are affected by the geological properties of the sites analyzed.

Table S5 presents the Raeq values of granite samples, ranging between 71 and 1895 Bq kg^{-1}, with a mean value of 289 Bq kg^{-1}. The vast majority of the granite samples (85 %) exhibit Raeq values below the globally accepted threshold of 370 Bq kg^{-1} [44]; (Fig. S3). This restriction enables the external dosage to be maintained at or below 1.5 mSv y^{-1} [1]. The average values for H_{in} and H_{ex} are 1.01 and 0.78, respectively, both of which fall below the globally permitted level. The range of values for H_{in} and H_{ex} is altered to 0.23 to 6.94 and 0.19 to 5.12, respectively. Notably, the mean values of H_{in} and H_{ex} in all granite samples exhibit no significant adverse effects, as they remain lower than the reference level set by the unit [45]; (Fig. S4).

Moreover, the highest Hin and Hex values observed in granite samples within the examined region may give rise to substantial health consequences as a result of exposure to gamma-rays, radon gas, and its decay products. Additionally, it is not advisable to employ the studied granite samples for construction purposes or as decorative elements in interior spaces. The mean value of (Iγ) for the granite samples is 1.08, which is comparable to the permissible limit [46], and the Min and Max values are 0.28 and 6.62, respectively (Fig. S4). The Iγ values indicate that there is no significant health risk associated with the granite samples observed in the surveyed locations. Therefore, these samples can be considered suitable for use in construction materials. The (D_{air}) values of the analyzed granite samples ranged from 41.31 to 682.56 nGy h^{-1}, with an a mean value of 126.05 nGy h^{-1}. The mean (D_{air}) value in the study area exceeds the global average of 59 nGy h^{-1} [1]. This finding suggests that the granites in the research region should not be used for construction materials or infrastructure. Table S6 presents the (AED_{out}) values, which range from 0.05 to 0.84 mSv y^{-1}, with a mean of 0.17 mSv y^{-1}, which is twice the approved worldwide value of 0.07 mSv y^{-1}

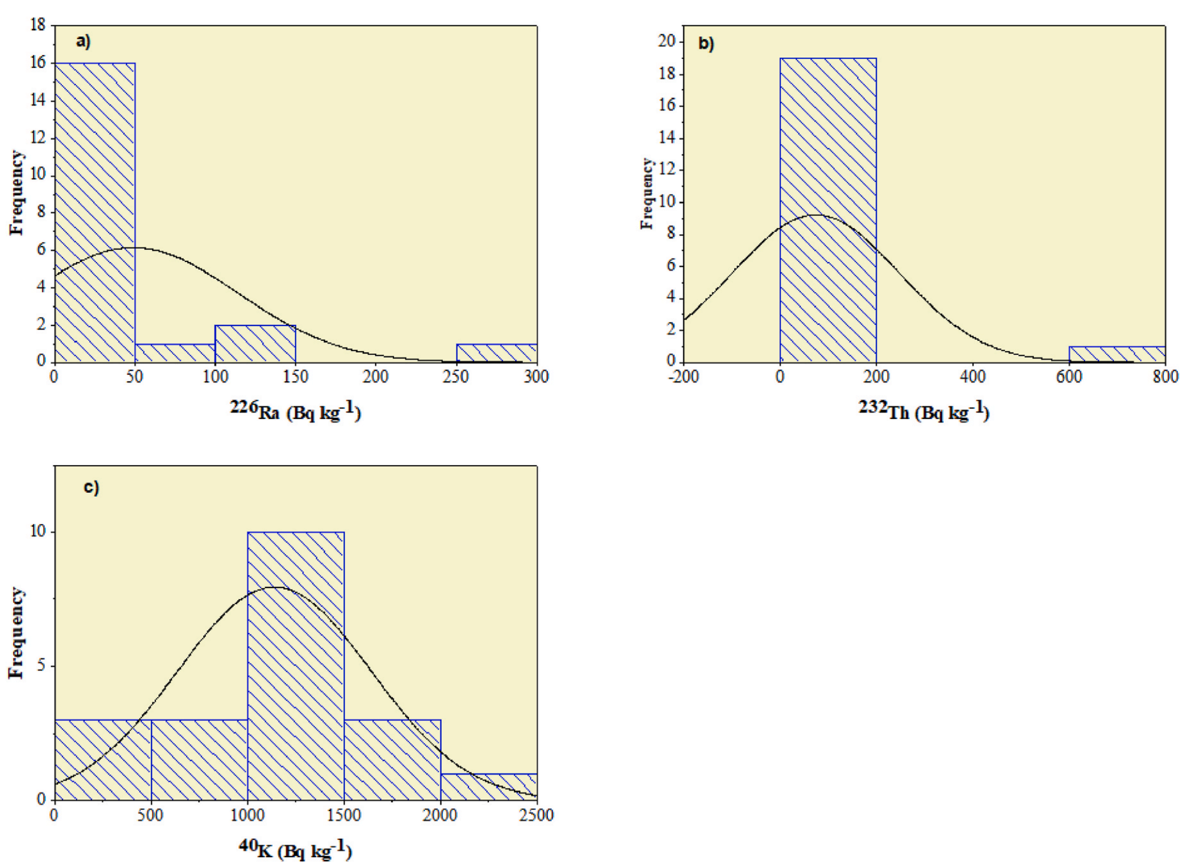

Fig. 2. Frequency distribution of a) ^{226}Ra, b) ^{232}Th, and c) ^{40}K activity concentrations in Abu Furad area.

[1]. Furthermore, the mean (AED_{in}) value is 0.68 mSv y^{-1}, surpassing the worldwide average of 0.41 mSv y^{-1} [1]. The AEDin values range between 0.20 and 3.35 mSv y^{-1}. The presence of heavy minerals in the granite, such as monazite, uraninite, and thorianite, can be attributed to these elevated doses. This indicates that prolonged exposure to low doses does not lead to adverse health effects such as tissue degeneration, DNA damage, cancer, or cardiovascular disease [47]. The adverse health effects will arise from prolonged exposure to emitted gamma radiation emitted by the granites studied throughout their lifespan. Exposure can occur through the utilization of various building materials and infrastructure fields made from these granites. The values for excess lifetime cancer risk (ELCR) ranged from 0.26×10^{-3} to 5.80×10^{-3}, with a mean of 0.97×10^{-3} for the granite samples, surpassing the approved value of 0.29×10^{-3} [48].

3.6. Statistical approach

3.6.1. Pearson correlation analysis (PC)

In this study, Pearson correlation analysis is utilized to identify robust connections and linear associations between activity concentrations of radionuclides and radiological hazard indicators in granite samples. The results categorize the linear relationships into four distinct groups. The first group represents a weak correlation (0.00–0.19), the second group shows a moderate correlation (0.2–0.39), the third group displays a strong correlation (0.4–0.79), and the fourth group exhibits a very strong correlation (0.8–1.00) [49]. Table S6 presents the positive correlations observed among the experimental parameters. The findings demonstrate that the radionuclides present in the samples under investigation originate from natural sources and that their geographic distribution in the environment remains undisturbed by external factors. Notably, a highly significant correlation exists between the activity concentrations of ^{226}Ra and ^{232}Th in the analyzed granite samples, indicating the presence of these isotopes in the examined granites derived from natural decay chains. Additionally, a weaker correlation is observed between ^{40}K and both ^{226}Ra and ^{232}Th. These correlations persist when considering the relationship between ^{226}Ra and ^{232}Th, and the variables associated with radiological hazard. It can be inferred that the presence of ^{226}Ra and ^{232}Th predominantly contributes to the radiological risks and the gamma rays emitted by the radioactive series in the granite samples.

3.6.2. Hierarchical cluster analysis (HCA)

Ward's approach was utilized in this study to attain cluster analysis. The application of Ward's approach establishes a connection between radioactive activity concentrations and radiological variables, allowing for the estimation of the Euclidean distance between them [50]. Fig. 3 illustrates that the data's dendrogram displays two prominent clusters. Cluster I consists of ^{226}Ra, which is correlated with a sub-cluster comprising ^{232}Th, Raeq, Hex, Hin, and Iγ. On the other hand, Cluster II encompasses ^{40}K and the remaining radiological characteristics. The results from Hierarchical Cluster Analysis (HCA) indicate a strong association between granite's radioactivity and concentrations of radium and thorium. These findings demonstrate a consistent agreement between the HCA data and the Pearson correlation.

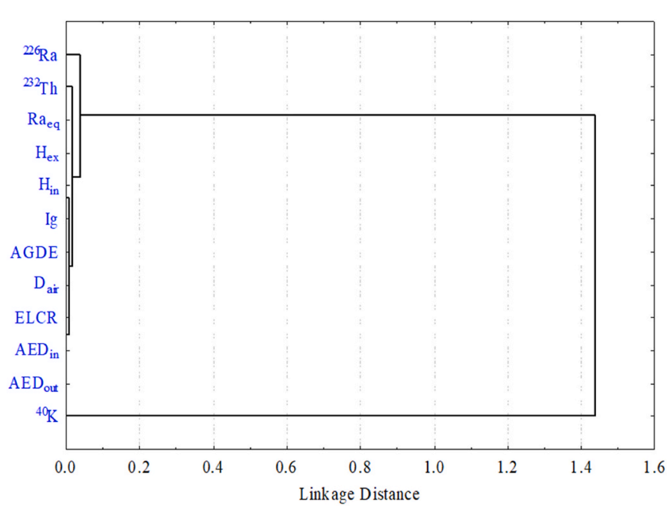

Fig. 3. The clustering analysis of the radiological parameters in Abu Furad area.

3.6.3. Principal component analysis (PCA)

This study utilized the PCA and varimax rotations to establish the matrix correlation between various components. Fig. S5 serves as an illustration of the components PC1 and PC2. In the PC1 loading, there is a significant loading associated with all radiological parameters, particularly the activity concentrations of ^{226}Ra and ^{232}Th. These two elements account for a high loading and explain 90.78 % of the variation. Consequently, in the study area, ^{226}Ra and ^{232}Th are the primary sources of naturally occurring radioactivity in granite. Conversely, in the PC2 load, ^{40}K exhibits a weak negative loading, and the variance explained is 8.86 %. The negative loading variance indicates that potassium does not have a substantial impact on the radiation exposure grade. Overall, the PC analysis reveals that the explained variance of the radioactive database is 99.72 %.

4. Conclusions

The novelty of this study lies in the assessment of radioactivity levels in granite rocks, which have potential uses as ornamental stones and across different infrastructure sectors. The average activity concentrations (±SD) for ^{226}Ra, ^{232}Th, and ^{40}K are 63 ± 71, 76 ± 170, and 1248 ± 532 Bq kg^{-1}, respectively. These values are notably higher than the global mean values reported by UNSCEAR (2010). Furthermore, an assessment was conducted on all radiological hazard parameters associated with the examined granite samples. The identification of elevated values surpassing accepted thresholds in these samples indicates the existence of radioactive minerals such as zircon, uranophane, and uranothorite within the granite rocks under investigation. A statistical analysis was performed to demonstrate the geological mechanisms responsible for the escalation in radioactivity concentration within granitic formations. Consequently, it is inferred that the granite rocks within the studied region pose potential risks to human well-being and are unsuitable for incorporation into diverse infrastructural projects, especially those involving construction materials.

Data availability statement

No Data associated in the manuscript.

Funding

This research was supported by Researchers Supporting Project number (RSP2024R351), King Saud University, Riyadh, Saudi Arabia.

Declaration of competing interest

The authors declare that they have no known competing financial interests or personal relationships that could have appeared to influence the work reported in this paper.

CRediT authorship contribution statement

Sherif A. Taalab: Conceptualization, Data curation, Formal analysis, Funding acquisition, Investigation, Methodology, Project administration, Resources, Software, Supervision, Validation, Visualization, Writing – original draft, Writing – review & editing. **Ahmed M. Ismail:** Conceptualization, Data curation, Formal analysis, Funding acquisition, Investigation, Methodology, Project administration, Resources, Software, Supervision, Validation, Visualization, Writing – original draft, Writing – review & editing. **W.M. El Maadawy:** Conceptualization, Data curation, Formal analysis, Funding acquisition, Investigation, Methodology, Project administration, Resources, Software, Supervision, Validation, Visualization, Writing – original draft, Writing – review & editing. **Kamal Abdelrahman:** Conceptualization, Data curation, Formal analysis, Funding acquisition, Investigation, Methodology, Project administration, Resources, Software, Supervision, Validation, Visualization, Writing – original draft, Writing – review & editing. **Mayeen Uddin Khandaker:** Conceptualization, Data curation, Formal analysis, Funding acquisition, Investigation, Methodology, Project administration, Resources, Software, Supervision, Validation, Visualization, Writing – original draft, Writing – review & editing. **Ahmed K. Sakr:** Conceptualization, Data curation, Formal analysis, Funding acquisition, Investigation, Methodology, Project administration, Resources, Software, Supervision, Validation, Visualization, Writing – original draft, Writing – review & editing. **Mohamed Y. Hanfi:** Conceptualization, Data curation, Formal analysis, Funding acquisition, Investigation, Methodology, Project administration, Resources, Software, Supervision, Validation, Visualization, Writing – original draft, Writing – review & editing.

Acknowledgments

This research was supported by Researchers Supporting Project number (RSP2024R351), King Saud University, Riyadh, Saudi Arabia.

Appendix A. Supplementary data

Supplementary data to this article can be found online at https://doi.org/10.1016/j.net.2024.05.017.

References

[1] UNSCEAR, Sources and Effects of Ionizing Radiation - Exposures of the Public and Workers from Various Sources of Radiation - UNSCEAR 2008 Report, 2010. New York, http://www.unscear.org/docs/reports/2008/09-86753_Report_2008_Annex_B.pdf.

[2] S. Sivakumar, A. Chandrasekaran, G. Senthilkumar, M. Suresh Gandhi, R. Ravisankar, Determination of radioactivity levels and associated hazards of coastal sediment from south east coast of Tamil Nadu with statistical approach, Iran J Sci Technol Trans A Sci 42 (2018) 601–614, https://doi.org/10.1007/s40995-017-0184-2.

[3] A. Abbasi, Radiation risk assessment of coastal biota from a quasi-Fukushima hypothetical accident in the Mediterranean Sea, Mar. Pollut. Bull. 194 (2023) 115363, https://doi.org/10.1016/j.marpolbul.2023.115363.

[4] M.A. Akpanowo, I. Umaru, S. Iyakwari, E.O. Joshua, S. Yusuf, G.B. Ekong, Determination of natural radioactivity levels and radiological hazards in environmental samples from artisanal mining sites of Anka, North-West Nigeria, Sci Afr 10 (2020) e00561, https://doi.org/10.1016/j.sciaf.2020.e00561.

[5] S. Pavlidou, A. Koroneos, C. Papastefanou, G. Christofides, S. Stoulos, M. Vavelides, Natural radioactivity of granites used as building materials, J. Environ. Radioact. 89 (2006) 48–60, https://doi.org/10.1016/j.jenvrad.2006.03.005.

[6] A.M. Abdel-Rahman, H.M. El-Desoky, B.N.A. Shalaby, H.A. Awad, A. Ene, M. A. Heikal, H. El-Awny, W. Fahmy, S.A. Taalab, H.M.H. Zakaly, Ultramafic rocks and their alteration products from northwestern allaqi province, southeastern Desert, Egypt: petrology, mineralogy, and geochemistry, Front. Earth Sci. 10 (2022), https://doi.org/10.3389/feart.2022.894582.

[7] A. El-Taher, M. Kamel, A. Tolba, G. Salaheldin, Evaluation of natural radioactivity and radiological hazards in basement rocks from Gabel Abu El-Hassan in the North Eastern Desert of Egypt by multivariate statistical approach with remote sensing data, Radiation Detection Technology and Methods 5 (2021) 15–26, https://doi.org/10.1007/s41605-020-00213-w.

[8] R. Abd El Rahman, S. Taalab, Z. Al Full, M. Mohamed, M. Sayyed, N. Almousa, M. Hanfi, Natural radionuclide levels and radiological hazards of khour abalea mineralized pegmatites, southeastern Desert, Egypt, Minerals 12 (2022) 353, https://doi.org/10.3390/min12030353.

[9] M.M. El Dabe, A.M. Ismail, M. Metwaly, S.A. Taalab, M.Y. Hanfi, A. Ene, Hazards of radioactive mineralization associated with pegmatites used as decorative and building, Material, Materials 15 (2022) 1224, https://doi.org/10.3390/ma15031224.

[10] A.M. El Mezayen, E.K. Abu Zeid, W.S. Hosny, M.G. El-Feky, S.M. Omar, S. A. Taalab, Geochemistry, mineralogy, and radioactivity of the Abu Furad area, central Eastern Desert, Egypt, Acta Geochimica 38 (2019) 307–326, https://doi.org/10.1007/s11631-018-0302-7.

[11] R.M. Anjos, N. Umisedo, A.A.R. da Silva, L. Estellita, M. Rizzotto, E.M. Yoshimura, H. Velasco, A.M.A. Santos, Occupational exposure to radon and natural gamma radiation in the La Carolina, a former gold mine in San Luis Province, Argentina, J. Environ. Radioact. 101 (2010) 153–158, https://doi.org/10.1016/j.jenvrad.2009.09.010.

[12] S.A. Taalab, W.H. Mohamed, S.A. Shetaia, M. Al Meshari, Y. Alzamil, A. Abanomy, A.R. Alyahyawi, A. El-Taher, Radiological and environmental hazards of granitic rocks in Wadi Faliq El Sahl and El Waar area, North Eastern Desert, Egypt, J. Environ. Sci. Health, Part A 58 (2023) 326–341. https://doi.org/10.1080/10934529.2023.2186650.

[13] J.M. Whitfield, J.J.W. Rogers, J.A.S. Adams, The relationship between the petrology and the thorium and uranium contents of some granitic rocks, Geochem. Cosmochim. Acta 17 (1959) 248–271, https://doi.org/10.1016/0016-7037(59)90099-7.

[14] J.W. Rogers, P.C. Ragland, Variation of Thorium and Uranium in Selected Granitic Rocks, vol. 25, 1961, pp. 99–109.

[15] S.A. Taalab, M. Al Meshari, Y. Alzamil, A. Abanomy, A.R. Alyahyawi, W. H. Mohamed, A. El-Taher, Radiological and ecological hazards evaluation of episyenite used as building materials, J. Radioanal. Nucl. Chem. 332 (2023) 2057–2075. https://doi.org/10.1007/s10967-023-08890-9.

[16] A. Abbasi, Natural radiation of chemical fertilisers and radiological impact on agriculture soil, J. Radioanal. Nucl. Chem. 331 (2022) 4111–4118, https://doi.org/10.1007/s10967-022-08470-3.

[17] B. Charrasse, A. Anderson, J.C. Mora, J. Smith, E. Cohenny, A.T.K. Ikonen, V. Kangasniemi, B. Zorko, Y. Bonchuk, L. Beaumelle, N. Gunawardena, V. Amado, L. Liptak, E. Leclerc, D. Telleria, Does the use of reference organisms in radiological impact assessments provide adequate protection of all the species within an environment? Sci. Total Environ. 658 (2019) 189–198, https://doi.org/10.1016/j.scitotenv.2018.12.163.

[18] M.P. Elless, E.S. Corporation, Chapter 25 Radionuclide-Contaminated Soils : A Mineralogical Perspective for Their Remediation, 2002.

[19] M.Y.M. Hanfi, M.S. Masoud, M.I. Sayyed, M.U. Khandaker, M.R.I. Faruque, D. A. Bradley, M.Y.A. Mostafa, The presence of radioactive heavy minerals in prospecting trenches and concomitant occupational exposure, PLoS One 16 (2021) e0249329. https://doi.org/10.1371/journal.pone.0249329.

[20] M.O. Barnett, P.M. Jardine, S.C. Brooks, H.M. Selim, Adsorption and transport of uranium(VI) in subsurface media, Soil Sci. Soc. Am. J. 64 (2000) 908–917, https://doi.org/10.2136/sssaj2000.643908x.

[21] N.A.M. Alsaif, M. Alotiby, M.Y. Hanfi, Al-Yousef, A. Haifa, B.M. Alotaibi, M. I. Sayyed, Comprehensive study of radiation shielding and mechanical features, J. Aust. Ceram. Soc (2021). https://doi.org/10.1007/s41779-021-00623-z.

[22] T. Taboada, A. Martinezcortizas, C. Garcia, E. Garciarodeja, Uranium and thorium in weathering and pedogenetic profiles developed on granitic rocks from NW Spain, Sci. Total Environ. 356 (2006) 192–206, https://doi.org/10.1016/j.scitotenv.2005.03.030.

[23] I.E. El Aassy, A.A. Nada, M.M. El Galy, M.G. El Feky, T.M. Abd El Maksoud, S. M. Talaat, E.M. Ibrahim, Behavior and environmental impacts of radionuclides during the hydrometallurgy of calcareous and argillaceous rocks, southwestern Sinai, Egypt, Appl. Radiat. Isot. 70 (2012) 1024–1033, https://doi.org/10.1016/j.apradiso.2012.03.018.

[24] A.M. El Mezayen, E.K. Abu Zeid, W.S. Hosny, M.G. El-Feky, S.M. Omar, S. A. Taalab, Geochemistry, mineralogy, and radioactivity of the Abu Furad area, central Eastern Desert, Egypt, Acta Geochimica 38 (2019) 307–326, https://doi.org/10.1007/s11631-018-0302-7.

[25] S. Monica, P.J. Jojo, M.U. Khandaker, Radionuclide concentrations in medicinal florae and committed effective dose through Ayurvedic medicines, Int. J. Radiat. Biol. 96 (2020) 1028–1037, https://doi.org/10.1080/09553002.2020.1767816.

[26] S. Arunima, R. Lekshmi, P.J. Jojo, K. Mayeen Uddin, A study on leaching of primordial radionuclides 232Th and 40K to water bodies, Radiat. Phys. Chem. 188 (2021) 109658, https://doi.org/10.1016/j.radphyschem.2021.109658.

[27] M. Iqbal, M. Tufail, S.M. Mirza, Measurement of natural radioactivity in marble found in Pakistan using a NaI(Tl) gamma-ray spectrometer, J. Environ. Radioact. 51 (2000) 255–265, https://doi.org/10.1016/S0265-931X(00)00077-1.

[28] MdJ. Abedin, MdR. Karim, S. Hossain, N. Deb, M. Kamal, MdH.A. Miah, M. U. Khandaker, Spatial distribution of radionuclides in agricultural soil in the vicinity of a coal-fired brick kiln, Arabian J. Geosci. 12 (2019) 236, https://doi.org/10.1007/s12517-019-4355-7.

[29] IAEA, Measurement of Radionuclides in Food and the Environment–Technical Reports, 1983. Vienna.

[30] A. Papadopoulos, G. Christofides, A. Koroneos, L. Papadopoulou, C. Papastefanou, S. Stoulos, Natural radioactivity and radiation index of the major plutonic bodies in Greece, J. Environ. Radioact. 124 (2013) 227–238, https://doi.org/10.1016/j.jenvrad.2013.06.002.

[31] M. Hasan, A. Hossain Chaity, A. Haydar, I. Ali, M. Uddin Khandaker, Elevated concentrations of terrestrial radionuclides in sand: an essential raw material used in Bangladeshi dwellings, Indoor Built Environ. 30 (2021) 1051–1061, https://doi.org/10.1177/1420326X20924835.

[32] A. Abbasi, S.F. Mirekhtiary, Risk assessment due to various terrestrial radionuclides concentrations scenarios, Int. J. Radiat. Biol. 95 (2019) 179–185, https://doi.org/10.1080/09553002.2019.1539881.

[33] F. Tuo, X. Peng, Q. Zhou, J. Zhang, Assessment of natural radioactivity levels and radiological hazards in building materials, Radiat. Protect. Dosim. 188 (2020) 316–321, https://doi.org/10.1093/rpd/ncz289.

[34] A.E. Abdel Gawad, M.S. Masoud, M.U. Khandaker, M.Y. Hanfi, Radiological hazards assessment associated with granitoid rocks in Egypt, Nucl. Eng. Technol. (2024), https://doi.org/10.1016/j.net.2024.01.032.

[35] J. Plášil, Oxidation-hydration weathering of uraninite: the current state-of-knowledge, J. Geosci. 59 (2014) 99–114, https://doi.org/10.3190/jgeosci.163.

[36] S. Avasarala, A.J. Brearley, M. Spilde, E. Peterson, Y.-B. Jiang, A. Benavidez, J. M. Cerrato, Crystal chemistry of carnotite in abandoned mine wastes, Minerals 10 (2020) 883, https://doi.org/10.3390/min10100883.

[37] C. Frondel, Systematic mineralogy of uranium and thorium, U.S. Geol. Sur. Bull 1064 (1958) 265–275, https://doi.org/10.3133/b1064.

[38] A.G. Darnely, Hot granite; Some general remarks, in: Y.T. Maurice (Ed.), Uranium in Granites, Geol. Surv. of Canada, 1982.

[39] M.G. El-Fekya, H.S. Mohammed, A.M. El-Shabasy, M.R. Ahmed, Y.K. Abdel-Monem, H.I. Mira, Mobilisation of radionuclides during uranium and gold processing of granitic rock at El-Missikate area, central Eastern Desert, Egypt, Int J Environ Anal Chem 00 (2021) 1–14, https://doi.org/10.1080/03067319.2021.1925262.

[40] R.L. Clark, R.C. Hickey, J.J. Butler, M.L. Ibanez, A.J. Ballantyne, Thyroid Cancer Discovered Incidentally during Treatment of an Unrelated Head and Neck Cancer: Review of 16 Cases, 1966, pp. 665–671.

[41] Y.A. Abdel-Razek, M.S. Masoud, M.Y. Hanfi, M.S. El-Nagdy, Effective radiation doses from natural sources at Seila area South Eastern Desert, Egypt, J. Taibah Univ. Sci. 10 (2016) 271–280, https://doi.org/10.1016/j.jtusci.2015.06.010.

[42] M.F. Raslan, On the Distinction between Uranophane and Beta-Uranophane from Some Uraniferous Granitoids in the Eastern Desert of Egypt, 2014.

[43] A.M. El Mezayen, E.M. Ibrahim, M.G. El-Feky, S.M. Omar, A.M. El-Shabasy, S. A. Taalab, Physico-chemical conditions controlling the radionuclides mobilisation in various granitic environments, Int J Environ Anal Chem 00 (2020) 1–17, https://doi.org/10.1080/03067319.2020.1729758.

[44] C. Sabbarese, F. Ambrosino, A.D. Onofrio, V. Roca, Radiological characterization of natural building materials from the Campania region (Southern Italy), Construct. Build. Mater. (2020) 121087, https://doi.org/10.1016/j.conbuildmat.2020.121087.

[45] R. Ravisankar, J. Chandramohan, A. Chandrasekaran, J.P. Prakash, I. Vijayalakshmi, P. Vijayagopal, B. Venkatraman, Assessments of radioactivity concentration of natural radionuclides and radiological hazard indices in sediment samples from the East coast of Tamilnadu , India with statistical approach, Mar. Pollut. Bull. (2015), https://doi.org/10.1016/j.marpolbul.2015.05.058.

[46] G. Senthilkumar, Y. Raghu, S. Sivakumar, A. Chandrasekaran, D. Prem Anand, R. Ravisankar, Natural radioactivity measurement and evaluation of radiological hazards in some commercial flooring materials used in Thiruvannamalai, Tamilnadu, India, J Radiat Res Appl Sci 7 (2014) 116–122, https://doi.org/10.1016/j.jrras.2013.12.009.

[47] USEPA, EPA Radiogenic Cancer Risk Models and Projections for the U . S . Population, 2011.

[48] A.A. Qureshi, S. Tariq, U. Kamal, S. Manzoor, C. Calligaris, A. Waheed, ScienceDirect Evaluation of excessive lifetime cancer risk due to natural radioactivity in the rivers sediments of Northern Pakistan, J Radiat Res Appl Sci 7 (2014) 438–447, https://doi.org/10.1016/j.jrras.2014.07.008.

[49] M.J. Abedin, M.R. Karim, M.U. Khandaker, M. Kamal, S. Hossain, M.H.A. Miah, D. A. Bradley, M.R.I. Faruque, M.I. Sayyed, Dispersion of radionuclides from coal-fired brick kilns and concomitant impact on human health and the environment, Radiat. Phys. Chem. 177 (2020) 109165, https://doi.org/10.1016/j.radphyschem.2020.109165.

[50] A.M.A. Adam, M.A.H. Eltayeb, Multivariate statistical analysis of radioactive variables in two phosphate ores from Sudan, J. Environ. Radioact. 107 (2012) 23–43, https://doi.org/10.1016/j.jenvrad.2011.11.021.